A Simple Model of the Australian West Coast Trough

JEFFREY D. KEPERT

Bureau of Meteorology Research Centre, Melbourne, Australia

ROGER K. SMITH

Meteorological Institute, University of Munich, Munich, Federal Republic of Germany

(Manuscript received 3 September 1991, in final form 11 December 1991)

ABSTRACT

The Australian west coast trough forms near the west coast in the easterly flow over Australia in the warmer months of the year. Its development and movement is the major synoptic influence on the weather in those months, particularly in the production of extreme maximum temperatures and subsequent "cool changes." This paper begins with a brief discussion of the climatology of the trough, followed by a case study. The main focus is on the development and interpretation of a simple dynamical model of the trough. The model is an adaptation of the linear diabatic equatorial β-plane models of Matsuno and of Gill for the particular situation of the trough. The study leads to a new hypothesis on the role of the sea breeze in the dynamics of the trough.

1. Introduction

Perhaps the feature of Perth's climate most appreciated by the summertime visitor is the frequent arrival of the afternoon sea breeze. This southwesterly breeze is known locally as the "Fremantle doctor" because it blows from the port of Fremantle, some 15 km to the southwest of the city. It provides welcome relief from maximum temperatures that average almost 30°C through the summer, and often exceed 35°C for periods of over a week. Shorter spells in the low 40s are common also.

The reason for these high temperatures is that, during the summer, much of the Australian subtropics lies between the subtropical ridge and the monsoon trough and is thereby under the influence of an easterly wind regime as shown in Fig. 1. Perth is located on the west coast and so, when not in a sea-breeze regime, it receives air that has spent several days over the hot arid continental interior.

The easterlies contain two significant troughs. The first is located to the east of the great Dividing Range along the east coast of Australia and heads southward from the Cloncurry region in central Queensland. The second lies generally inland of the west coast in the mean but shows considerably greater amplitude and day-to-day variation in position than the eastern trough. This is the topic with which this paper is most concerned.

Corresponding author address: Jeffrey D. Kepert, BMRC, P.O. Box 1289K, Melbourne, Victoria 3001, Australia.

The importance of the west coast trough to Perth's summertime temperatures lies in its effect on the sea breeze. It is widely recognized that when the trough is offshore, then the sea breeze, if it develops at all, will be weak, will arrive in the late afternoon, and will fail to penetrate very far inland. In any case, the result is a hot day for the coastal communities. If conditions conspire to keep the trough offshore for several consecutive days, the result is a heat wave. On the other hand, when the trough is inland, a vigorous sea breeze develops comparatively early in the day. In this case, the maximum temperature will be near or below average.

The influence of the trough on the sea breeze is easy to understand, at least qualitatively. The sea-breeze flow is driven by the pressure gradient created by the onshore differential heating, its direction modified by the Coriolis force. In the case of the Australian west coast, this makes the sea breeze a southwesterly. To the west of the trough axis, the pressure-gradient force is directed toward the northeast, and so the synoptic pressure gradient acts to reinforce the sea breeze. Once the sea breeze reaches the trough axis, however, it runs head on into the northeasterly flow from off the continent and is thereby prevented from penetrating much farther inland.

Another factor that may assist the sea breeze in penetrating to the trough axis is that the axis can be expected to be a region of significant upward motion. As air parcels approach the trough from central Australia, their relative vorticity changes sign from anticyclonic to cyclonic, and their planetary vorticity becomes increasingly cyclonic. Their absolute vorticity therefore

© 1992 American Meteorological Society

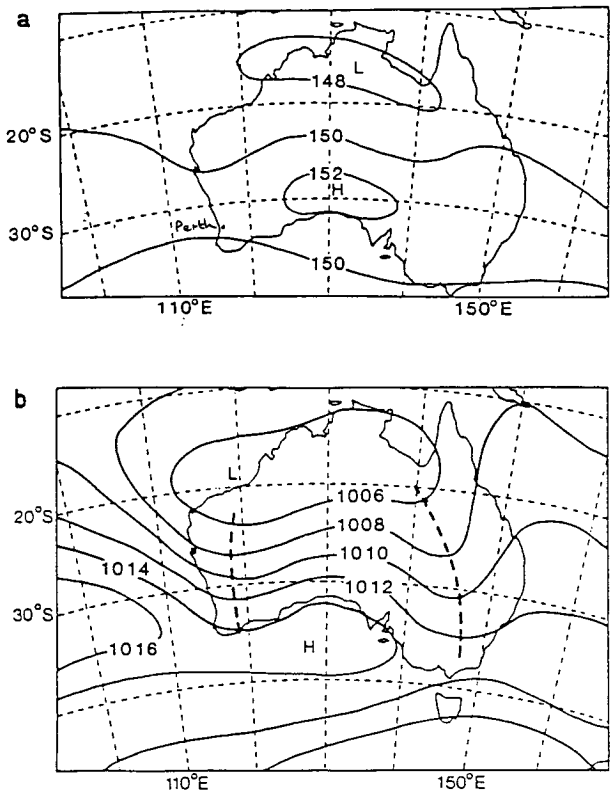

FIG. 1. Monthly mean charts of (a) 850-hPa height and (b) mean sea level pressure for the Australian region for January.

becomes markedly more cyclonic. Such parcels will not conserve potential vorticity, because of the intense continental heating, but to the extent that they do, they can be expected to undergo vertical stretching, particularly near the trough axis. This would tend to favor the location of the upward branch of the sea-breeze circulation in this area.

The trough is important to forecasting for reasons other than wind, temperature, and associated factors such as fire danger. A deep, mature west coast trough may develop afternoon thunderstorms to the east of the axis, if other factors are also favorable. Typically, these storms have high bases, generally between 2.5 and 4 km above ground level. Furthermore, mature troughs that have persisted near the west coast for several days before moving eastward frequently produce extensive areas of overcast low stratus along the south coast in their wake. This normally occurs in the evening after they become mobile.

Although at their peak importance in the summer months, west coast troughs can occur throughout much of the year. The first for the season generally occurs early in spring, typically early September. Thereafter, they gradually become a more dominant feature of the flow, reaching their peak intensity in mid-to-late summer. During the autumn they become progressively less common. Forecasting experience indicates that the more severe thunderstorms are associated with springtime troughs rather than summer, presumably because the continental troposphere tends to be both more baroclinic and moister in the transitional season.

The physical process forcing the trough is believed to be the pressure reduction due to the intense heating of the easterly airstream over the continent. A gentle escarpment parallels the west coast from south of about 30°S, increasing in height to a peak of only 582 m some 70 km southeast of Perth. For this reason, and the fact that troughs are most prevalent during the hotter months, it is unlikely that orography is a major forcing influence.

The first part of this paper presents a case study of a typical "trough sequence." The latter part is concerned with the formulation and solution of a simple dynamical model of the trough.

2. A case study: 13–18 February 1987

This study is based on operational analysis charts obtained from the Bureau of Meteorology, Western Australian Regional Forecasting Centre in Perth, with some minor reanalysis to take account of late data and to correct minor errors. All times are given in Western Australian standard time (WST), which is 8 h ahead of universal time coordinated (UTC). The mean sea level charts for the period are displayed in Fig. 2.

The period begins with the end of the previous trough's life cycle. At 0900 on the 13th (Fig. 2a), the previous trough had broadened and moved into the east of the state ahead of a weak cold front that brushed along the south coast, bringing a few showers and areas of drizzle to those parts. The previous trough was shown by upper wind data to extend to about 850 hPa at this stage. A high pressure cell to the west was extending a rapidly growing ridge along the south coast. The strength of the ridging is shown by the surface pressure at Cape Leeuwin, which rose 5.6 hPa in the 15 h from 0900 to midnight.

By 0900 the following morning (Fig. 2b), the high pressure cell had moved to the south of Cape Leeuwin and was directing a fresh easterly airstream over much of the state, with Perth's gradient wind being measured by the 0600 balloon flight as 105° at 13 m s^{-1}. A broad weak trough lay parallel to and somewhat inland of the west coast. By 1500 this had deepened and moved closer to the east, and the 1800 balloon flight showed Perth's gradient wind to have swung around to 80° at 13 m s^{-1}, showing the trough to be then offshore.

The 0900 analysis for the 15th (Fig. 2c) shows that the trough had deepened markedly and was virtually coincident with the coast in southern parts, although still inland in the north. Lower-tropospheric streamline analyses show that the trough was still well marked at 850 hPa. By 1500 the trough had drifted slightly inland, all west coastal observations had a sea breeze, and the

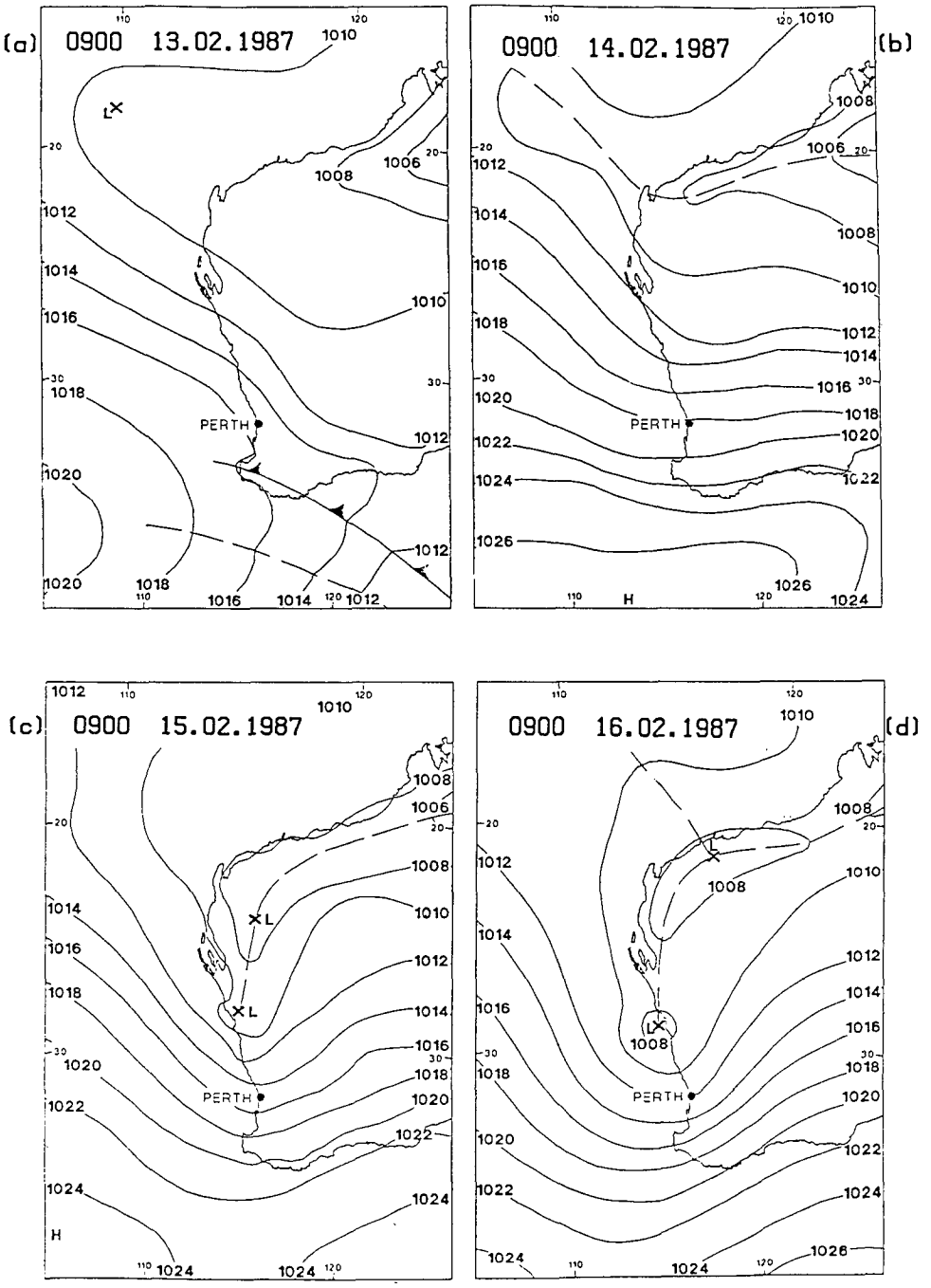

FIG. 2. Mean sea level isobaric analyses for the period 0900 WST 13 February 1987–0900 WST 18 February 1987.

temperature at Perth was 30°C. The trough still extended vertically to 850 hPa, and at this level, a weak closed circulation had developed in the vicinity of Shark Bay. At midnight, Perth's temperature remained high at 29°C, and the gradient wind was 90° at 20 m s^{-1}.

The following morning showed that the low, previously located at 850 hPa, had extended to the surface and moved southward (Fig. 2d). The trough axis lay well offshore of the southern part of the west coast, and a tight pressure gradient prevailed along this region. At 1500 the low had split in two, a rather unusual occurrence, although the upper-air data confirmed the offshore position of the trough. Perth's temperature at this time was 38°C, and nowhere to the south of the low was experiencing a sea breeze. The depth of the

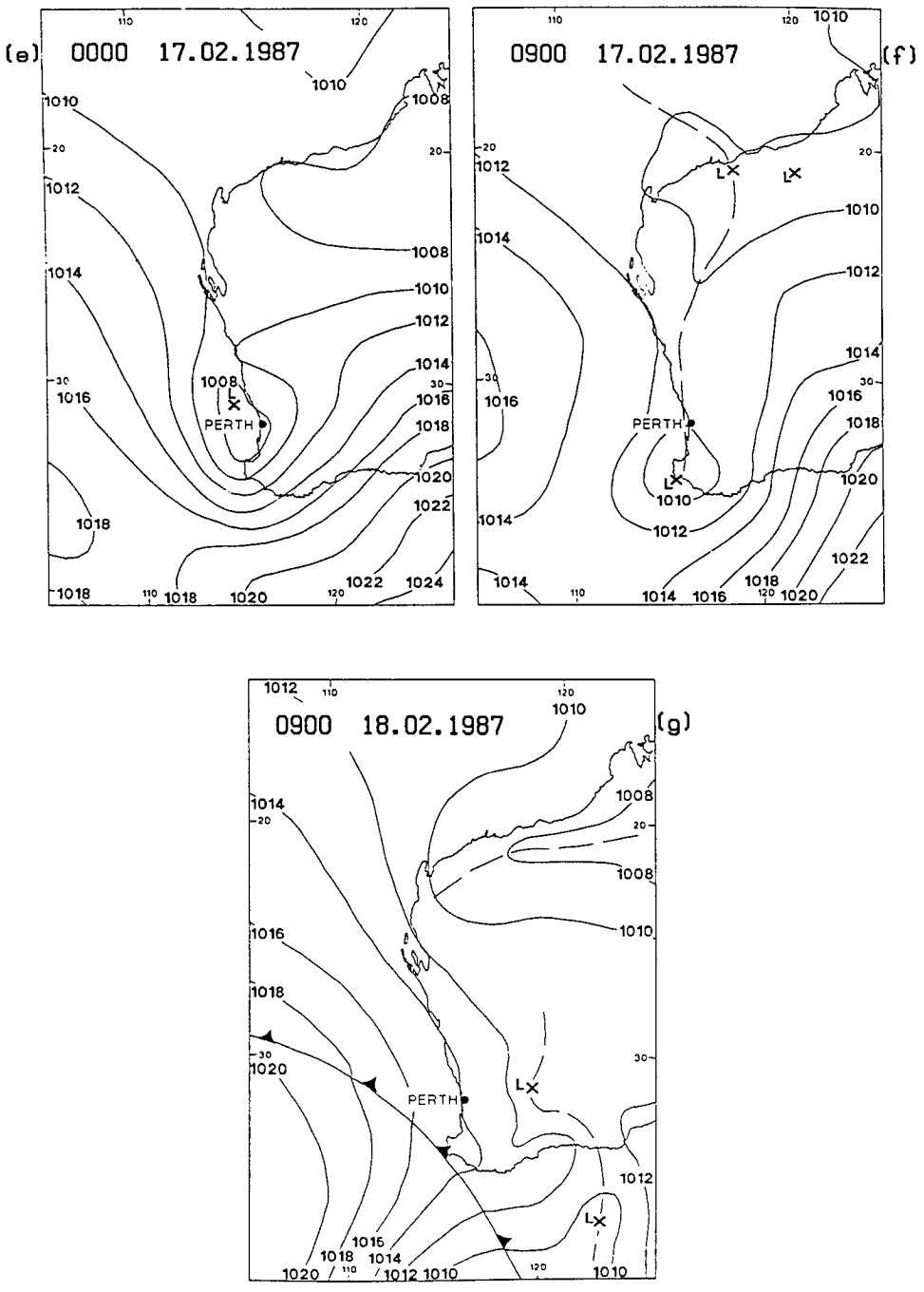

FIG. 2. (*Continued*)

heating is indicated by the 1800 radiosonde flight from Perth airport, which showed that the lapse rate from the surface to 600 hPa differed from a dry adiabat by only 1°C. By midnight only the offshore low remained, and this had migrated farther to the south (Fig. 2e). This southward movement of lows that form in the trough is observed almost invariably and is presumably due to warm-air advection to the south of the low causing the pressure to fall there, while cold-air advection to the north causes the pressure to rise. It is also of interest to note that at midnight, Perth's temperature was still very warm at 32°C.

At 0900 on the 17th (Fig. 2f), the low was located to the south of Cape Leeuwin in a markedly broadened trough. The low then proceeded to migrate along the south coast, and at 1500 the trough was located well

inland. The 1500 observation shows patchy rain and thunderstorm activity to the east of the trough, and extensive low stratus was observed along those parts of the south coast to the west of the trough in the evening.

The movement of the trough then continued, with the 0900 chart for the 18th (Fig. 2g) showing a remarkable similarity to that of the 13th, as the sequence began anew.

To conclude this description, it should be emphasized that this example shows only one of the many forms that west coast troughs can take. Many spend more time offshore than in this example, and it is also uncommon for them to develop embedded lows as in this example. A more detailed discussion of the climatology of the west coast trough may be found in Watson (1980).

3. The model

Our aim is to construct a model that is as simple as possible, while still retaining the essential features of the trough. It is hypothesized that the main forcing agent is the strong heating resulting from the passage of air over the hot interior of the continent, with the minor topography near the western coast playing a relatively unimportant role. Indeed this was the conclusion drawn by Watson (1984) and by the modeling study of Fandry and Leslie (1984), but see the note in Section 4c regarding the latter. This study extends and sheds further light on Fandry and Leslie's model results.

Probably the simplest dynamical framework in which to study atmospheric heating and cooling is to use the shallow-water equations, with the forcing provided by a distribution of mass sinks and sources, corresponding to diabatic heating and cooling, respectively. This technique was used to advantage by Matsuno (1966) and Gill (1980) in a study of equatorial waves, and it was further applied by Silva Dias et al. (1983), Heckley and Gill (1984), and Gill and Philps (1986).

The above studies were all of tropical phenomena, the equations being applied on an equatorial β plane. This interest in the tropics reflects the fact that most tropical atmospheric disturbances have diabatic heating as an essential ingredient in their dynamics, while, in contrast, many midlatitude synoptic-scale phenomena can be simulated to a reasonable degree of accuracy by models that neglect all diabatic sources and sinks. This present study differs from those above in that it applies the heating parameterization in the subtropics, and so a midlatitude β plane is appropriate.

Another feature of the tropical models is that they generally include some simple dissipative processes, such as a linear friction and cooling. The reason for this inclusion is that the steady-state equations are otherwise degenerate, whereupon meaningful conclusions cannot be drawn from the model. This problem does not arise in the application described here, and dissipation is not strictly necessary. However, it will be included for the purposes of comparison, and it will be shown that it has a dramatic and physically unrealistic influence on the form of the solution.

The basic model configuration consists of two layers of homogeneous fluid with densities ρ_1 and ρ_2 (suffixes 1 and 2 apply to the upper and lower layers, respectively). A uniform easterly geostrophic flow $U_2 = -U$, ($U > 0$) is prescribed in the lower layer, while the upper layer is either at rest or has a uniform geostrophic flow U_1 that may be easterly or westerly. Heating or cooling of the lower layer would correspond with a local reduction or increase of the volume of denser fluid ρ_2. This may be represented by prescribing a mass sink or source in the lower layer. It is immaterial whether the mass is thought of as being removed or added through the lower boundary, or as being converted to upper-layer fluid with density ρ_1. The upper layer is taken to be infinitely deep and is therefore essentially passive, except that the prescribed flow therein determines the mean meridional slope of the interface between the two layers. Momentum transfer between the upper and lower layers is not permitted. The coordinate axes (x, y) are chosen with the usual convention that x points eastward and y northward and since the results are compared with observations in the Southern Hemisphere, the Coriolis parameter f is taken to be negative. Planetary-vorticity gradients are taken into account by setting $f = f_0 + \beta y$ with f_0 and β constants. This is the usual β-plane approximation. Orography may be taken into account provided it is sufficiently low so as not to affect the basic-state solution, but only a small perturbation to it.

The shallow-water equations are linearized about the foregoing basic state and a potential vorticity equation is derived governing perturbations thereto. In nondimensional form, the potential-vorticity equation takes the form

$$\left(\frac{\partial}{\partial t} - \frac{\partial}{\partial x}\right)(\nabla^2 - \mu^2)\eta + (\nu\nabla^2 - \tau\mu^2)\eta + Q\frac{\partial \eta}{\partial x} = \mu^2\left(m + \frac{\partial D}{\partial x}\right) \quad (3.1)$$

where η is the perturbation depth of layer 2, nondimensionalized with respect to the undisturbed depth H of this layer at $y = 0$, and $Q = \bar{\beta} - \mu^2\delta$ is a nondimensional measure of the basic-state potential-vorticity gradient in layer 2. The key parameters are μ, the horizontal length scale L in units of the Rossby radius of deformation, $L_R = (g'H/f_0)^{1/2}$, where $g' = g(\rho_1 - \rho_2)/\rho_2$ is the reduced gravity, $\bar{\beta} = \beta L^2/U$ is a scaled value of β; and δ, a measure of the velocity difference between the upper and lower layers, normalized by U. Two additional parameters are ν, a linear friction coefficient, and τ, a Newtonian cooling coefficient, suitably

nondimensionalized. The functions $m(x)$ and $D(x)$ on the right-hand side are a nondimensional measure of the rate of mass removal or conversion to the upper layer, and the nondimensional variation of orography, respectively.

Choosing an appropriate value for δ is more difficult. As the shear is always westerly, δ must be positive. If the easterlies are much deeper than the trough, as is often the case in summer, then δ will be small. As the baroclinicity increases and the upper tropospheric westerlies extend downward toward the trough layer, δ will increase. This has important consequences for the sign of the basic-state potential-vorticity gradient Q in that there is a critical value of δ for which this changes sign and eastward-propagating Rossby-like waves become possible. As δ increases further it may then reach a second critical value where the rate of eastward propagation is sufficient to overcome the basic easterly flow.

We shall return to this point later. In the meantime, a reasonable upper bound for δ can be determined from Fig. 1, which shows very light winds above the trough. Taking then U_1 to be zero gives $\delta = 1$. Toward the southern extremity of the trough where the surface easterlies are shallower would give larger δ, but a value of 2, corresponding to a westerly layer of equal strength immediately above the easterly layer would be extreme.

Typical values of the parameters in the present context are $U = 10\ \text{m s}^{-1}$, $f_0 = 10^{-4}\ \text{s}^{-1}$, $\beta = 2 \times 10^{-11}\ \text{m}^{-1}\ \text{s}^{-1}$, $g' = 2\ \text{m s}^{-2}$, $H = 2000$ m, $L = 10^6$ m (10^3 km), and $L_R = (g'H)^{1/2}/f_0 = (2 \times 10^3)^{1/2}/10^{-4} = 630$ km, giving $\mu^2 = 2.5$ and $\bar{\beta} = 2$.

4. Model solutions and discussion

a. One-dimensional steady-state solutions

The simplest possible flow configuration is one dimensional ($\partial/\partial y = 0$) and steady ($\partial/\partial t = 0$) with no frictional dissipation or Newtonian cooling ($\nu = \tau = 0$). The corresponding form of the quasigeostrophic equation (3.1), rearranged a little and integrated from $-\infty$ to x, is

$$\frac{\partial^2 \eta}{\partial x^2} - (\mu^2 + Q)\eta = -\mu^2(\phi + D) \qquad (4.1)$$

where $\phi(x) = \int_{-\infty}^{x} m dx$.

As $\mu^2 + Q > 0$, this has homogeneous solutions

$$\eta = \exp[\pm(\mu^2 + Q)^{1/2} x].$$

Numerical solutions to the forced equation will be discussed shortly. In the case of a simple forcing, however, analytic solutions are possible also. The simplest forcing corresponds with a uniform mass transfer of unit rate between $x = 0$ and $x = 1$, and zero transfer elsewhere, coupled with flat topography, $D = 0$. Then the forcing function ϕ in (4.1) is given by

$$\phi(x) = \begin{cases} 0, & x > 1, \\ x - 1, & 0 < x < 1, \\ -1, & x < 0. \end{cases} \qquad (4.2)$$

The solution for η in the three regions $x < 0$, $0 \leqslant x \leqslant 1$, and $x > 1$ which is bounded for all x and has continuous derivatives at $x = 0$ and 1 is

$$\eta(x) = \begin{cases} \dfrac{\mu^2}{s^2}\left[\dfrac{1}{2s}(1 - e^{-s})e^{sx} - 1\right], & x < 0, \\ \dfrac{\mu^2}{s^2}\left\{\dfrac{1}{2s}[e^{-sx} - e^{s(x-1)}] + x - 1\right\}, & 0 \leqslant x \leqslant 1, \\ \dfrac{\mu^2}{s^2}\left[\dfrac{1}{2s}(1 - e^{s})e^{-sx}\right], & x > 1, \end{cases} \qquad (4.3)$$

where $s = (\mu^2 + Q)^{1/2}$. This solution is shown in Fig. 3a. Note that it is antisymmetric about $x = 0.5$. It is interesting to note also that the response length scale is

$$\frac{L}{s} = \left[\frac{\bar{\beta}}{L^2} + \frac{1}{L_R^2}(1 - \delta)\right]^{-1/2}. \qquad (4.4)$$

Streamlines of the flow $y = y(x)$ satisfy approximately

$$\frac{dy}{dx} = \frac{v}{U},$$

where v is the northward velocity component of the perturbation. Since v is calculated geostrophically from η, the streamlines have the same shape as the profiles of η. All that is needed to interpret profiles as streamlines is to put a leftward-pointing arrow on them and adjust the ordinate scale appropriately.

b. Maritime cooling

Perhaps the most obvious feature of the solution shown in Fig. 3a is that the "trough" near the west coast ($x = 0$) differs from the Australian west coast trough in that there is no southerly component in the flow over the sea. This defect may be overcome in a variety of ways, and this subsection considers the effect of incorporating a maritime cooling in the forcing, modeled by placing a mass source off the west coast.

The overall reduction in η as x goes from ∞ to $-\infty$ follows easily from (4.1); as $x \to -\infty$, $\partial^2\eta/\partial x^2 \to 0$ and so $\eta(-\infty) = (\mu^2/s^2)\phi(-\infty)$. This suggests that a reasonable choice for m would satisfy $\int_{-\infty}^{\infty} m dx = -\phi(-\infty) = 0$, thus ensuring that, in the model, streamlines return at $x = -\infty$ to the latitude from which they originated at $x = \infty$.

A simple mass-transfer function satisfying this constraint is

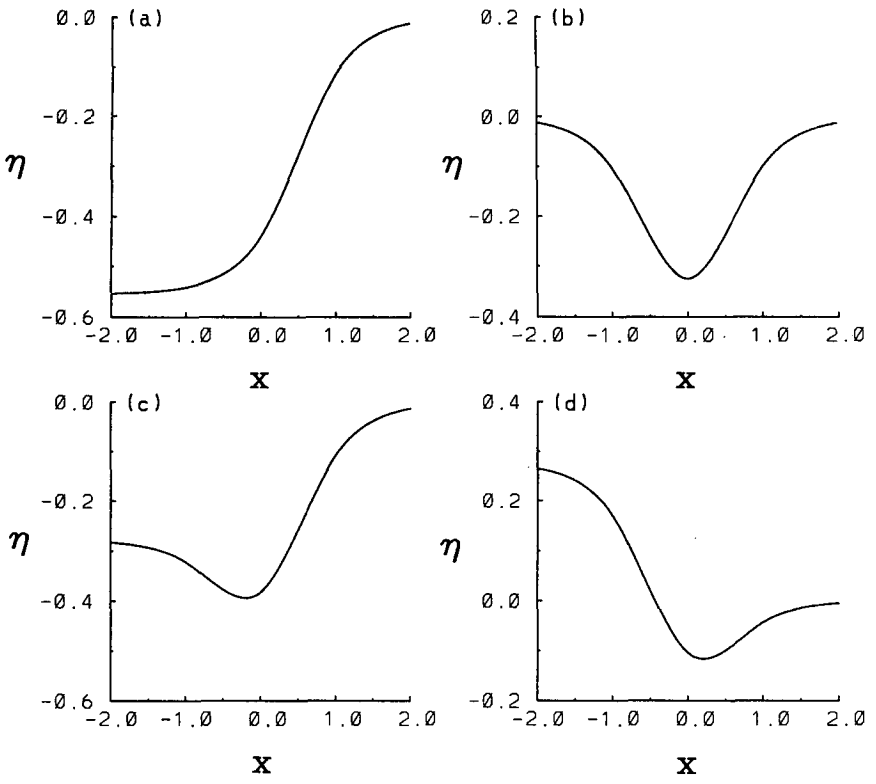

FIG. 3. Model response to a variety of simple forcing functions, showing the nondimensional layer depth $\eta(x)$. (a) The simplest forcing of Eq. (4.2). (b) The forcing with standard maritime cooling [Eq. (4.5)]. (c) As for (b), but with half the cooling. (d) As for (b), but with twice the cooling. Parameter values are $\mu^2 = 2.5$, $\beta = 2$, and $\delta = 0$.

$$m(x) = \begin{cases} 0 & x > 1 \\ 1 & 0 < x < 1 \quad \text{land} \\ -1 & -1 < x < 0 \quad \text{cool sea} \\ 0 & x < -1 \end{cases} \tag{4.5}$$

and this yields the solution shown in Fig. 4.

Figure 3 also displays solutions obtained with m altered from the above between $x = 0$ and $x = -1$ (the cool sea). If the maritime cooling is halved, the trough moves offshore to approximately $x = -0.17$ (Fig. 3c). When the cooling is doubled, the opposite situation prevails and the trough moves onshore (Fig. 3d). These shifts in trough position remain qualitatively the same for other values of μ^2, δ, and $\bar{\beta}$, provided that the length scale over which the model responds, $(\mu^2 + Q)^{1/2}$, is not too much greater than the length scale of mass addition, equal here to unity. It is clear, therefore, that the relative magnitudes of heating over the land and cooling over the sea can play a role in locating the trough.

This mirrors one facet of the real trough's behavior. In late summer the land and sea are both near their annual maximum temperatures, and so heating is strong and cooling is relatively weak. Then, the trough is much more likely to form offshore and remain there for several days, thereby providing heat-wave conditions for coastal towns. In spring, however, when the heating is much weaker and the sea is close to being at its coldest, the trough is much more likely to form over the land and rarely persists offshore.

Although the aforementioned model is appealing in that it provides a simple explanation of seasonal trends in the favored position of the trough, it is likely that

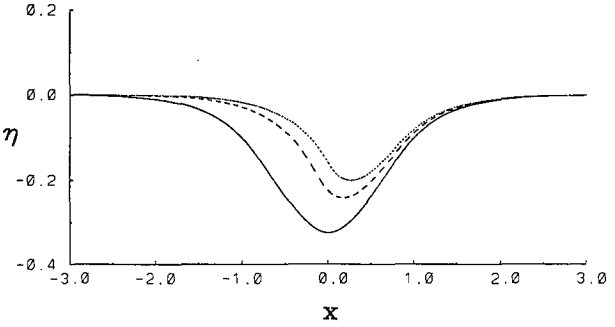

FIG. 4. Model response to the forcing with maritime cooling spread over a nondimensional distance $1/\gamma$ [Eq. (4.6)]. Solid curve is for $\gamma = 1$, dashed curve for $\gamma = 4$, and the dotted curve represents the limit as $\gamma \to \infty$.

other factors are important also. For example, one of the several factors that forecasters in Perth look for when considering possible trough movement is the approach of a cold front from the west, since a trough will frequently move inland ahead of such a front. With the seasonal change in position of the subtropical ridge, these fronts are far more likely to be located near Western Australian latitudes in spring than in summer, and this factor would also play a role in determining the preferred position of the trough.

The precise details of the nature of the maritime cooling in the real trough are likely to be much more complex than those of the heating over the land, since the relevant physical processes will include the development of internal boundary layers and sea-breeze circulations. In the absence of a sea breeze, one would expect a relatively thin internal boundary layer to form as the hot, well-mixed continental air flows over the ocean. The highly stable nature of such a configuration would tend to substantially reduce the heat fluxes from the hot air into the sea. [See, for example, Mulhearn (1981) and Garratt and Ryan (1989).] A sea-breeze circulation would transport cooler air to an altitude of a 1000 m or so near the coast and thereby enhance the cooling in this area. This would also have the effect of making the air farther west less stably stratified near the surface than would be the case in the absence of a sea breeze, and so stronger cooling farther offshore would also be favored by the existence of a sea breeze near the coast. Thus, a sea breeze will enhance the surface heat fluxes over the full length scale of the trough, even though the trough length scale is larger than that of the sea breeze.

To explore the direct influence of a strong, near-coastal sea breeze on the trough location, the model response was determined for a mass-transfer function given by

$$m(x) = \begin{cases} 0 & x > 1 \\ 1 & 0 < x < 1 \qquad \text{land} \\ -\gamma & -1/\gamma < x < 0 \quad \text{cool sea} \\ 0 & x < -1/\gamma \end{cases} \tag{4.6}$$

with several values of γ.

For $\gamma = 1$, this is just the situation shown in Fig. 3. Figure 4 shows the result obtained for a variety of values of γ. It is clear that as γ increases, that is, as the maritime cooling is progressively concentrated near the coast, the trough is displaced farther inland. In addition, it is reduced slightly in amplitude and is sharpened on its western flank.

In summary, we have found that different configurations of maritime cooling can alter the position of the trough. Increasing (decreasing) the overall cooling, but leaving its distribution unaltered, moves the trough eastward (westward), as illustrated in Fig. 3. If the total cooling is kept constant, but its effect is concentrated near the coast, then the trough is displaced eastward (Fig. 4). It is of interest to note that a doubling of the strength of the maritime cooling (Fig. 3d) places the trough axis almost coincident with that obtained by providing the same net cooling, but concentrated over only one-fourth of the amount of sea (Fig. 4).

c. *The induced westerly flow*

Climatological atlases of maritime surface flow such as Sadler et al. (1987) and Ramage et al. (1972) show that the monthly mean flow up to several hundred kilometers off the west coast of Western Australia during summer has a cross-isobaric component of around 45°, which is unusually large for maritime flow. This suggests that some mechanism other than friction is producing a westerly ageostrophic component in the flow. This suspicion is supported by a consideration of the **Q** vectors [$\mathbf{Q} = D(\nabla\theta)/Dt$] near the coast, which would be expected to point toward the land and thereby imply a low-level westerly ageostrophic flow.

This westerly component can be estimated in the context of the current one-dimensional form of the model here, as $\delta/\delta y \equiv 0$ implies that u carries all of the divergence. The one-dimensional vorticity and height equations are

$$\frac{\partial \zeta}{\partial t} - \frac{\partial \zeta}{\partial x} - \frac{1}{R_0}\frac{\partial u}{\partial x} + \bar{\beta} v = 0$$

$$\frac{\partial \eta}{\partial t} - \frac{\partial \eta}{\partial x} + \delta v + \frac{1}{R_0 \mu^2}\frac{\partial u}{\partial x} = -m(x).$$

Adding the first to ∇^2 of the second, and calculating v and η geostrophically gives

$$\frac{1}{R_0}\left(\frac{1}{\mu^2}\nabla^2 u - u\right) = -\frac{\partial m(x)}{\partial x} + (\beta + \delta\nabla^2)\eta,$$

which is in some sense an analog of the usual quasi-geostrophic ω equation. This is straightforward to solve by finite-difference methods. For the forcing functions (4.2) and (4.5) the solution yields the flows shown in Fig. 5, which confirms the discussion above.

d. *Two-dimensional solutions*

A motivation for extending our theory to two dimensions is to explore the detailed structure of the troughs that result when the forcing is a more realistic representation of Australia's topography and heating. Another is to compare the response of the single-layer model to various types of forcing with the response of the Fandry and Leslie (1984) model, which has a different heating parameterization. The relationship between the heating parameterizations in the two models is explored also, and it is shown that the Fandry and Leslie parameterization is less realistic at the western coastline. This has an effect on the positioning of their model west coast trough.

It is not easy to find exact solutions to the two-dimensional steady-state version of (3.1) when forced by more realistic functions $m + dD/dx$; accordingly the solutions presented in the following are all numerical. The numerical algorithm was verified against an analytic solution for a nonphysical forcing. The boundary conditions used were $\eta \to 0$ upstream ($x \to \infty$), $\partial\eta/\partial x \to 0$ downstream ($x \to -\infty$), and $v \to 0$ as $y \to \pm\infty$.

In their paper, Fandry and Leslie (1984; henceforth referred to as FL) parameterized heating and cooling, respectively, as sources and sinks of cyclonic potential vorticity, while here it is parameterized by the removal and addition of mass. The relationship between these methods is easy to see; inspection of (3.1) shows that mass addition ($m > 0$) acts directly as a source of cyclonic potential vorticity. In other words, FL's total forcing R_s is equivalent to $\phi + D$ in the model described here, whereupon it is possible to determine the response of this model to FL's forcing function. A sample solution is presented in Fig. 6 for their total forcing (orography and heating). The actual forcing functions used were

$$\left.\begin{aligned}
&\text{orography}\\
&D(x, y)\\
&\quad = b(y)\begin{cases} 0.625\{1 - \tanh[2(x+1)]\}, & -2 \le x < 0,\\ 3\exp[-8(x-2)^2], & 0 \le x \le 2,\\ 0, & \text{otherwise.}\end{cases}\\
&\text{western heating}\\
&\phi_W(x, y)\\
&\quad = b(y)\begin{cases} -2\{1 - \tanh[3(x+1)]\}, & -2 \le x \le 0,\\ 0, & \text{otherwise.}\end{cases}\\
&\text{eastern heating}\\
&\phi_E(x, y)\\
&\quad = b(y)\begin{cases} -2.56\exp[-8(x-1)^2], & -2 \le x \le 2,\\ 0, & \text{otherwise.}\end{cases}
\end{aligned}\right\} \tag{4.7}$$

where

$$b(y) = \begin{cases} 0.5\{1 - \tanh[4(y-1)]\}, & y > 0,\\ 0.5\{1 + \tanh[4(y+1)]\}, & y \le 0.\end{cases} \tag{4.8}$$

In these equations an apparent sign error in FL has been corrected. Furthermore, the same relative effects of orography and heating as FL have been retained. It should be noted that FL use a lapse rate γ to convert a temperature gradient to a height gradient and state [their Eq. (2.22)] that "potential vorticity change . . . is proportional to $\nabla(T_B/\gamma)$." The choice of this proportionality constant will clearly determine whether orography or surface heating has the dominant effect on the model response to a forcing that tries to represent both factors, but the appropriate value is difficult to assign. Unfortunately, without further comment, FL select a value of 0.1 for this constant and so their conclusion that heating is the dominant forcing mechanism, rather than orography, for the formation of the west coast trough, cannot strictly be drawn from their model results.

As the model is quasigeostrophic, the isopleths of height, or pressure, drawn in Fig. 6, also represent streamlines. The sum of the perturbation flow and a uniform easterly with dimensionless velocity -1 is shown. The perturbations to the easterly flow have been exaggerated to clearly show the troughs, although the linear model of course requires the perturbation amplitudes to be small.

The troughs are virtually coincident with those of FL. As both models are linearized about a basic easterly, it is not meaningful to compare the amplitude of the troughs. An interesting difference appears in the decay length scales, with their Figs. 6, 9, and 10 showing longer decay scales than obtained here. This discrepancy can be explained by the following simple analysis.

If we let the depth of the FL upper layer, (in their notation) $D_1 \to 0$, or equivalently, $F_1 \to \infty$, then it is easy to deduce from their Eq. (2.6) that

$$\nabla^2\varphi_2 - \left(-\frac{\beta}{U_2}\right)\varphi_2 = -R_s, \tag{4.9}$$

where φ_2 is their perturbation streamfunction for the lower layer. Recalling that their $U_2 < 0$ for an easterly, this clearly has evanescent solutions with length scale $(-\beta/U_2)^{1/2}$. This is in contrast to the decay length scale here of $[\beta + \mu^2(1 - \delta)]^{1/2}$, which corresponds most closely to their $(\beta + F)^{1/2}$. For the actual numbers used in the respective simulations, numerical values for these are (FL) 1.414 and (here) 1.105, which accord with the discrepancy noted above. Thus, the difference is due to the choice of $\delta = 0$ for Fig. 6. Had $\delta = 1$ been chosen, the figures would have been more comparable.

It is clear from these results that the second, westerly layer included by FL is redundant from the point of view of creating troughs. In the real trough, the presence and movement of synoptic-scale features in the mid-to-upper-tropospheric westerlies has an important effect on the day-to-day variation in the trough. The upper westerlies are not, however, necessary for its existence.

An interesting feature of the FL western heating function is the "step" in the profile at the western coast. In the context of mass sources and sinks, this is the

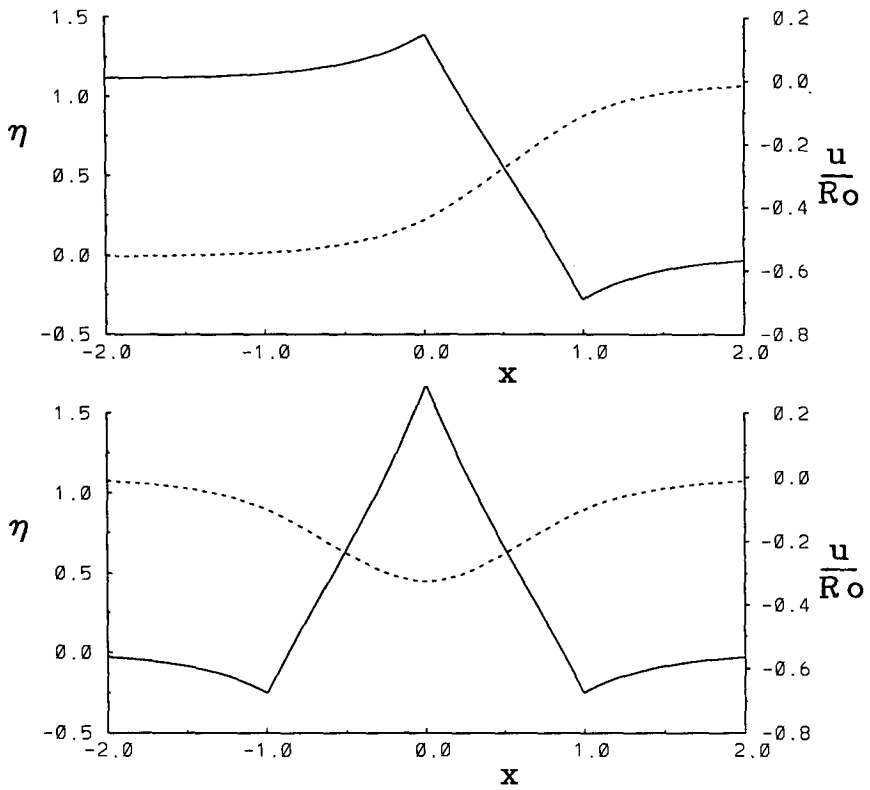

FIG. 5. Model response $u(x)/R_0$ (solid) for the simple forcing functions Eq. (4.2) (top) and Eq. (4.5) (bottom). Also shown for comparison is $\eta(x)$ (dotted).

physical equivalent of an infinitely strong source of zero width, located on the coast. It is difficult to postulate a mechanism that could effectively undo the effects of heating over the entire continent in such an abrupt fashion. As was discussed earlier, the magnitudes of mass addition and removal rates nearest the coast have the strongest effect on trough location. If, as seems more plausible, the cooling is spread over some distance from the coast, the model trough would be relocated some distance to the west. This matter is discussed further in the next section.

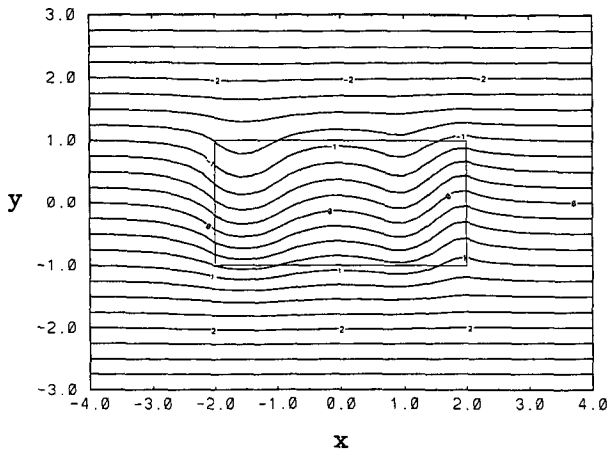

FIG. 6. Two-dimensional calculation showing isolines of layer depth in response to the total forcing $D + \phi_E + \phi_W$ used by Fandry and Leslie (1984).

e. *Effects of friction and cooling*

Here the analysis of section 4a is extended to explore the effects of including "Newtonian cooling" τ and "Rayleigh friction" ν on the one-dimensional steady-state solutions. It will be shown that they have a dramatic effect on the form of the solutions obtained.

The relevant form of (3.1) is

$$\frac{\partial^3\eta}{\partial x^3} - \nu\frac{\partial^2\eta}{\partial x^2} - (\mu^2 + Q)\frac{\partial\eta}{\partial x} + \tau\mu^2\eta = -\mu^2 m. \quad (4.10)$$

Throughout this section, only the simplest forcing m, as given by (4.2), will be used.

Since the linear dissipative processes are not directly derived from a physical model, it is difficult to decide on appropriate values for the coefficients ν and τ. Indeed, it is quite usual not to distinguish between the two. Gill (1980) sets them equal and uses 0.1 in his calculations, while discussing the "small-nu limit" in

much of his text. Matsuno (1966) similarly sets them to be equal at 0.2, while Zebiak (1982) claims that 0.3 produces the "best" results in his study of the El Niño. We have used either 0 or 0.1 for each of ν and τ in cases where a specific value was required. Physically, ν and τ are inverse time scales, nondimensionalized by L/U, which is on the order of 1 day. It takes several days for an air parcel to cross Australia in an easterly stream [3000 km $(10\ \mathrm{m\ s^{-1}})^{-1}$] and so a choice of $1/\tau$ and $1/\nu$ to be 2 or 3 days would be a sensible upper bound to the value of the dissipative time scale. This is in accordance with the values in the papers cited above.

Exact solutions were found by arguments similar to those described above. Numerical solutions were obtained also. If we restrict the parameters ν, τ, μ^2, and $\bar{\beta}$ to "reasonable" values, the family of solutions to (4.10) can be divided into three categories. These are the result of different types of homogeneous solutions that in turn are determined by the sign and type of the roots to the characteristic polynomial.

1) NO NEWTONIAN COOLING: $\tau = 0$

If $\mu^2 + Q = 0$ also, it is easy to see that there are no bounded solutions. For $\mu^2 + Q > 0$, we require to solve

$$\frac{\partial^2 \eta}{\partial x^2} - \nu \frac{\partial \eta}{\partial x} - (\mu^2 + Q)\eta = -\mu^2 \phi, \qquad (4.11)$$

which has homogeneous solutions

$$\exp\left\langle \frac{1}{2} x\{\nu \pm [\nu^2 + 4(\mu^2 + Q)]^{1/2}\} \right\rangle.$$

Reasonable values of the parameters give $\mu^2 + Q \gg \nu$, making this expression approximately $\exp[\frac{1}{2}x(\mu^2 + Q)^{1/2}]$. Accordingly, the solution to the forced equation will differ from those without Rayleigh friction only by a slight modification of the response length scales.

2) NEWTONIAN COOLING: $\tau > 0$, $\mu^2 + Q = 0$

Then the discriminant of the characteristic (cubic) polynomial is positive so the polynomial has one real root and two complex conjugate ones. Using Spiegal (1968, p. 32) it is easy to show that the real part of the complex roots is positive, while, for typical values [i.e., $\mu^2 = O(1)$, $\nu = O(0.1)$], the real root is negative. This leads to the type of solution shown in Fig. 7 where there is a decaying oscillation downstream of the forcing. As $Q + \mu^2 = 0$ requires unrealistically large δ for the Australian west coast trough, this family of solutions is included only for completeness of the discussion.

3) NEWTONIAN COOLING: $\tau > 0$, $\mu^2 + Q > 0$

The discriminant in this case is a complicated expression, but numerical experiments show that the form of the solution depends only marginally on whether ν is 0 or 0.1. In the former case it is negative, showing there are three real roots, two positive and one negative and smaller. In this case the solution to (4.10) has a longer response scale on the downstream side than on the upstream. An example of this type is shown in Fig. 7.

We conclude from these calculations that the Newtonian cooling rate τ plays an important role in determining the form of the solution, while the strength of Rayleigh friction ν has very little effect. These conclusions were confirmed by numerical solutions of the full equation (4.10).

When Newtonian cooling is implemented, a genuine trough forms, as shown in Fig. 7. This trough is "offshore" in each case. In neither case, though, is it particularly realistic, as the response length scale is much too large, being many times the length scale of the forcing. (For comparison, the calculations for Fig. 7 used values $\mu^2 = 2.5$ and $\bar{\beta} = 2$, as for Fig. 3.)

An interesting side effect of the Newtonian cooling is that it forces $\eta \to 0$ as $x \to -\infty$. The reason for this is easily seen: integrating (4.10) from $-\infty$ to ∞ and applying boundary conditions we obtain

$$\tau \int_{-\infty}^{\infty} \eta dx = -\int_{-\infty}^{\infty} m dx, \qquad (4.12)$$

which is finite, when $\eta(-\infty) = 0$.

In summary, then, Rayleigh friction ν makes barely any difference to the solution obtained, while Newtonian cooling τ alters it radically. The actual form the solution takes depends on whether $\mu^2 + Q$ is zero or not. In either case, however, when reasonable values of μ^2 and $\bar{\beta}$ are used, the decay scales of the solution tend to be much larger than the extent of the forcing m. This is at considerable variance with experience.

In this model, as in others, the choice of a Newtonian cooling is an attempt to simply represent a variety of physical processes, although its precise relationship to any of them must inevitably be somewhat nebulous.

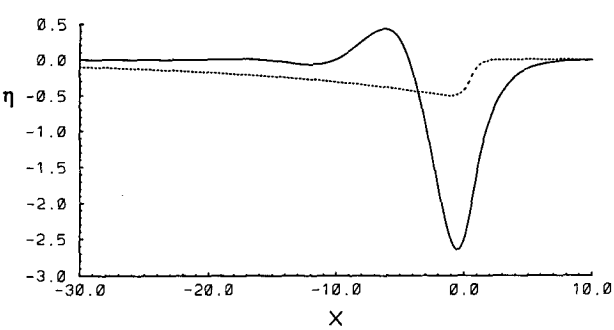

FIG. 7. Model response to the simplest forcing, but including Newtonian cooling ($\tau > 0$). Solid line is the case for which $\mu^2 + Q = 0$; dotted line for the case $\mu^2 + Q > 0$.

It certainly lacks the clear physical interpretation that could be attached to an offshore mass source earlier.

f. Time-dependent solution

Equation (3.1) was solved numerically for the unsteady one-dimensional case with no viscous or thermal damping. The algorithm used was implicit in time, a straightforward extension of the well-known Crank–Nicholson method.

The first experiment used the simplest prototype heating function, given by (4.2). The solution (not shown) consists of two parts:

(i) a disturbance that is advected westward by the basic flow with (dimensionless) velocity -1, and
(ii) the familiar steady solution that remains anchored to the forcing region.

As the dimensional time scale $T = L/U = 10^6/10$ s is approximately 1 day, it follows that the most interesting part of this solution is the first two time divisions or so, before the two aforementioned components have become separated. During this period the trough forms initially inland and makes its way offshore after a couple of days or so, a result that accords well with the real atmosphere.

In Western Australia, a trough is often observed to form in the first instance in a southeasterly flow of comparatively short overland trajectory. As the associated high pressure cell in the eastern Indian Ocean progresses eastward into the Great Australian Bight region, the basic flow becomes more easterly, and this leads to a progressive lengthening of the overland trajectory upstream of the trough over the next few days. Figure 8 shows the result of an attempt to model this behavior. Here the forcing function (4.2) is progressively imposed between $t = 0$ and $t = 1$. From then until $t = 3$, the extent of the heating is increased until it has a nondimensional length 3. At the same time, the strength of the cooling is increased to balance the heating according to $\int_{-\infty}^{\infty} m dx = 0$. After $t = 3$, the forcing is held constant at its value at $t = 3$, that is, there is unit heating between $x = 0$ and $x = 3$ with a cooling rate of 3 between $x = -1$ and $x = 0$.

The above result, together with the earlier steady-state solutions, suggests that, in the real atmosphere, the maritime cooling is an important ingredient in the maintenance of a mature quasi-steady trough, though its effect may not be as important during the first day or two of the life of a trough.

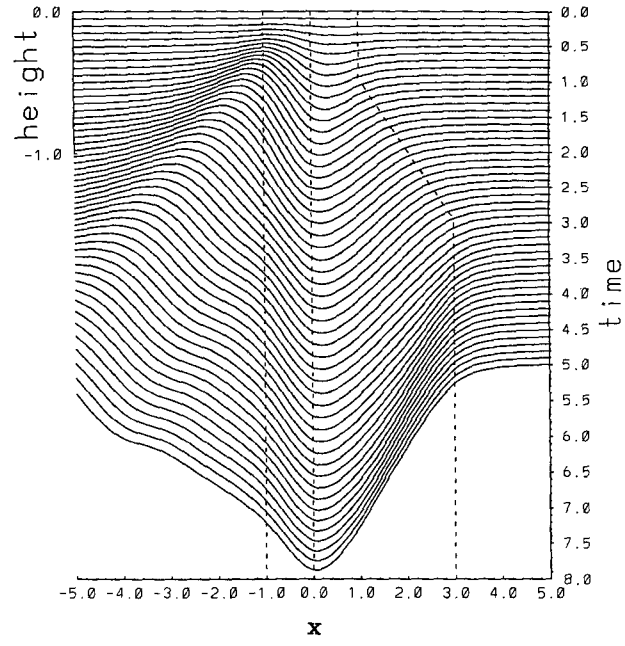

FIG. 8. Time–depth diagram showing the response $\eta(x, t)$ for the forcing with increasing lateral extent. The dashed lines show the extent of the heating as a function of time. The nondimensional depth scale is shown on the upper left of the figure.

5. Further discussion and conclusions

The foregoing model studies confirm the hypothesis that surface heating is capable of producing a trough that qualitatively resembles those observed in the real atmosphere. Further, they show that orography also could play a role, but the fact that troughs are most dominant in the warmer part of the year suggests that this is a less important mechanism.

Our calculations point to the importance of maritime cooling in the maintenance of a steady-state trough, with heating alone not being capable of producing a realistic trough. The relative strengths and distributions of the heating and cooling in the overall forcing then determines the position of the model trough. This positioning accords well with the actual seasonally preferred positions for west coast troughs.

The heating is generally very deep and strong in summertime trough situations, and the only mechanism capable of inducing a similar rate of cooling to sufficient depth to correspond to a similar-sized mass source in the model would be the sea breeze. If the sea breeze were not to develop, as when the offshore flow is too strong, an internal boundary layer would form in the offshore flow and inhibit heat transfer from the air to the sea. This leads us to hypothesize that the sea breeze is an important component of the cooling mechanism, both in transporting cool air aloft near the coast and also in reducing the stability farther west and thereby enhancing the surface heat fluxes there. It therefore seems likely that the extent of sea-breeze development will influence trough location.

It is well known to forecasters in the Perth region that major factors affecting the timing, inland penetration, and strength of the sea breeze are the depth,

position, and expected movement of the trough. It seems likely from the above discussion that the sea breeze's role in enhancing cooling to the west of the trough axis helps also to determine the position of the trough.

This could apply both during "heat waves," when the trough is offshore and virtually stationary, and at best just a weak sea breeze reaches the coastal fringe late in the afternoon, or, in the opposite case, when the trough is well inland and the sea breeze along the west coast develops shortly after sunrise, has penetrated perhaps 100 km inland by the afternoon, and remains strong for several hours after sunset. The hypothesis is that in the former case, a weak sea-breeze–like circulation exists for much of the day to the west of the trough but only barely becomes strong enough to reach the coast late in the afternoon. In the latter case, it extends the effect of maritime cooling across the coastal strip and up to the trough axis and thereby helps keep the trough inland.

Another factor that seems to be of importance in the trough's dynamics follows from the idea of large values of δ producing a reversal on the basic-state potential-vorticity gradient, and hence the possibility of eastward-propagating pseudo-Rossby waves. As δ is a measure of the westerly shear, or equivalently, the zonal temperature gradient, it can be expected to vary on a day-to-day basis. A cold front approaching the continent from the southwest, as in the case study, would increase the temperature gradient and the associated midlevel trough would "push" the subtropical ridge at those levels northward, thereby allowing westerlies at lower levels and increasing δ. These two effects are linked, of course, through the thermal wind equation. These increases in δ would result in a strongly reversed gradient of potential vorticity and allow the trough to propagate upstream to the east. This movement inland is exactly what is observed to happen when a Southern Ocean front approaches the continent, as was shown in the case study.

The idea of a reversed potential-vorticity gradient is supported by the discussion in Hoskins et al. (1985) of the lower-tropospheric potential-vorticity patterns produced by surface temperature anomalies. Briefly, a surface hot anomaly produces a cyclonic (negative in the Southern Hemisphere) potential-vorticity anomaly, and a cool surface is associated with an anticyclonic PV anomaly. It is clear that if the continent becomes sufficiently hot, this could result in a reversal of the usual potential-vorticity gradient. In reality, both the synoptic effect above and this smaller-scale behavior may be important in causing a sufficient large reversal of the PV gradient to allow upstream propagation of the trough. Given the major impact that trough position has in forecasting for the populous west coast, it seems that testing of this hypothesis, both by field study and by more sophisticated modeling, would be of considerable benefit as an improved understanding of the relationship between the trough and the sea breeze could only enhance the overall forecast performance.

Troughs could also be produced by pure heating (with no maritime cooling) if linear dissipative functions (Newtonian cooling and Rayleigh friction) were also included in the model. However, these troughs had unrealistic length scales, and their form was found to be very sensitive to the setting of the other model parameters, so this approach was rejected.

The unsteady equations were solved also and the response of the model to a "switch on" of the forcing was examined. It was found that the trough first developed inland, before migrating toward the coast. Again, this is a feature of some real troughs. It was found that a realistic trough could be formed from a "heating" alone for the first couple of days, without the need for a maritime cooling. This may also be of importance to the real atmosphere.

Solving the two-dimensional steady-state equations enabled a comparison with the model of Fandry and Leslie (1984), and further light was shed on the physical meaning of their results.

The full (nonquasigeostrophic) model was also solved and this suggested that and ageostrophic westerly component may exist along the coastline, which would be in accordance with the ageostrophic flow predicted by a simple **Q**-vector argument.

Finally, it should be reiterated that this study has led to new hypotheses on the role of the sea breeze in forcing the west coast trough, and especially in determining its quasi-steady position, as well as a model for its eventual movement inland as a Rossby wave propagating against the basic flow on a strongly reversed potential-vorticity gradient.

Acknowledgments. Jeff Kepert was supported by a Bureau of Meteorology scholarship while undertaking this study. He would also like to thank his former colleagues at the Western Australian Regional Forecasting Centre for their helpful discussions.

One of the reviewers pointed out the quasigeostrophic solution for u in section 4c, which was simpler than our original calculation.

Finally, but not least, we thank Ulrike Beye at the University of Munich who skillfully typed the manuscript.

REFERENCES

Fandry, C. B., and L. M. Leslie, 1984: A two-layer quasigeostrophic model of summer trough formation in the Australian subtropical easterlies. *J. Atmos. Sci.*, **41**, 807–818.

Garratt, J. R., and B. F. Ryan, 1989: The structure of the stably stratified internal boundary layer in offshore flow over the sea. *Bound.-Layer Meteor.*, **47**, 17–40.

Gill, A. E., 1980: Some simple solutions for heat-induced tropical circulations. *Quart. J. Roy. Meteor. Soc.*, **106**, 447–462.

——, and P. J. Philps, 1986: Nonlinear effects on heat-induced cir-

culation of the tropical atmosphere. *Quart. J. Roy. Meteor. Soc.*, **112,** 69–91.

Heckley, A. W., and A. E. Gill, 1984: Some simple analytical solutions to the problem of forced equatorial long waves. *Quart. J. Roy. Meteor. Soc.*, **110,** 203–217.

Hoskins, B. J., M. E. McIntyre, and A. W. Robertson, 1985: On the use and significance of potential vorticity maps. *Quart. J. Roy. Meteor. Soc.*, **111,** 877–946.

Matsuno, T., 1966: Quasigeostrophic motions in the equatorial area. *J. Meteor. Soc. Japan,* **44,** 25–43.

Mulhearn, P. J., 1981: On the formation of a stably stratified internal boundary layer by advection of warm air over a cooler sea. *Bound.-Layer Meteor.*, **21,** 247–254.

Ramage, C. S., F. R. Miller, and C. Jeffries, 1972: *Meteorological Atlas of the International Indian Ocean Expedition Vol 1: The Surface Climate of 1963 and 1964.* National Science Foundation/U.S. Government Printing Office, Washington D.C.

Sadler, J. C., M. A. Lander, A. M. Hori, and L. K. Oda, 1987: *Tropical Marine Climate Atlas Vol 1: Indian Ocean and Atlantic Ocean.* Dept. of Meteorology, University of Hawaii. Honolulu, Hawaii.

Silva Dias, P. L., W. H. Schubert, and M. DeMaria, 1983: Large-scale response of the tropical atmosphere to transient convection. *J. Atmos. Sci.*, **40,** 2689–2707.

Spiegel, M. R., 1968: *Mathematical Handbook of Formulas and Tables.* Schaum's Outline Series, McGraw-Hill Book Company, 270 pp.

Watson, I. D., 1980: A dynamical climatology of the Australian west coast trough. Ph.D. thesis, University of Western Australia. [Available from the Librarian, University of Western Australia, Perth, Australia.]

——, 1984: Density change in an Australian west coast trough. *Aust. Meteorol. Mag.*, **32,** 123–129.

Zebiak, S. E., 1982: A simple atmospheric model of relevance to El Niño. *J. Atmos. Sci.*, **39,** 2017–2027.